Rapid, Direct Measurement of Bulk RF Power Deposition using Free Induction Decay Acquisitions

Leeor Alon[1,2], Assaf Tal[1,2], Giuseppe Carluccio[1,2], Cem M. Deniz[1,2], Karthik Lakshmanan[1,2], Daniel K. Sodickson[1,2], and Christopher C. Collins[1,2]
[1]*Department of Radiology, Bernard and Irene Schwartz Center for Biomedical Imaging, New York University School of Medicine, New York, NY, United States,*
[2]*Sackler Institute of Graduate Biomedical Sciences, New York University School of Medicine, New York, NY, United States*

INTRODUCTION: Monitoring of global RF power deposition is necessary to ensure patient safety. Recent developments allow global RF power deposition to be estimated rapidly in vivo for single and multiple transmit MRI systems [1]. These RF power-monitoring systems measure the forward and reflected power and calculate the net injected RF power into the patient. In practice however, losses in the transmit chain electronics, coil structure, radiated energy, variable coupling of the subject to the coil, and other factors may prevent accurate estimates of the amount of power that is coupled into the phantom or patient. In this work, we utilized a novel method of experimentally measuring the RF energy deposited into the phantom/subject using the frequency distribution observed from single pulses rather than by monitoring power. Two free induction decays (FIDs) are acquired (2 second acquisition each), before and after RF energy is delivered to the phantom/patient. The FIDs are fourier transformed and the first moments with respect to frequency are calculated. In principle, the difference between the first moments of each FID corresponds to the average temperature change (ΔT) and total RF power deposited. Results are given in phantoms and in-vivo.

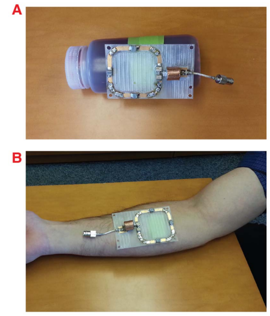

Figure 1. Loop coil used for RF heating experiments positioned on top of the imaged phantom (A) and the forearm of the subject (B).

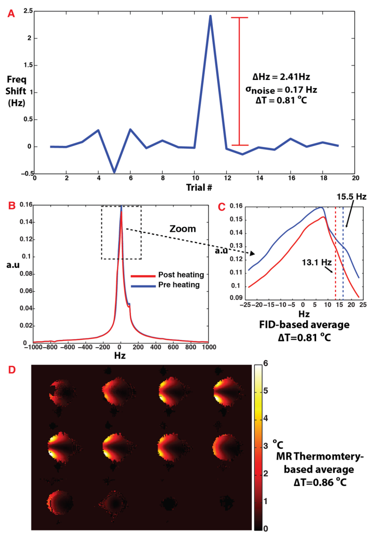

Figure 2. Phantom experiment. A. Difference in first moment of two adjacent FIDs. The first ten trials correspond to no heating, trial 11 corresponds to the difference in frequency due to heating and trials 12-19 correspond to no heating, respectively. B. Two FIDs corresponding to pre- and post-heating. C. Zoom onto the center frequency showing the shift in first moment. D. MR thermometry of the phantom.

THEORY: Pennes bio heat equation describes the spatial distribution and temporal evolution of temperature as [2]:

$$\rho C\frac{dT}{dt} = \nabla\cdot(k\nabla T) + [\rho_{blood} w c_{blood}(T - T_{core})] + Q_m + SAR\rho \quad (1).$$

where ρ, C, and k are the tissue density (kg/m^3), heat capacity (J/kg/C), and thermal conductivity (W/m/C), respectively, T is local temperature, Q_m is the heat generated from metabolism, and SAR (W/kg) is the driving force for temperature rise defined as: $SAR = \frac{\sigma|E|^2}{2\rho}$, where **E** is the induced electric field (V/m), and σ is the electrical conductivity (S/m). When the heating duration is short, Eq. (1) can be simplified to: $SAR = C\frac{\Delta T}{\Delta t}$ (2) where Δt is the RF heating time-interval. ΔT in MR can be monitored using the proton resonance frequency (PRF) shift method [3] that linearly relates ΔT to frequency of nuclear precession. As result, the first moment of the absolute value of the spectrum of an FID applied before and after heating quantifies the average ΔT deposited by the RF coil:

$$\Delta T_{avg} = \frac{1}{\alpha\cdot\omega}\cdot\left[\frac{\int_{-BW/2}^{BW/2} f(x)_{FID1}\cdot x\cdot dx}{\int_{-BW/2}^{BW/2} f(x)_{FID1}\cdot dx} - \frac{\int_{-BW/2}^{BW/2} f(x)_{FID2}\cdot x\cdot dx}{\int_{-BW/2}^{BW/2} f(x)_{FID2}\cdot dx}\right] \quad (3).$$

FIDs 1 and 2 represent the acquisitions before and after SAR exposure, respectively, f(x) represents the amplitude of the spectrum at each frequency point x, ω is the Larmor frequency, BW is the bandwidth of the spectrum, and α is the proton's frequency shift coefficient which is typically 0.01 PPM/deg C [3]. Equation (3) is reliant on the fact that the thermal dose is applied for a short duration of time and that the effect of temperature on PRF is much larger than that from other non-thermal changes (e.g., B_0 drift). Once the average ΔT is measured using FIDs 1 and 2, the thermal dose is calculated as $SAR = C_{avg}\frac{\Delta T_{avg}}{\Delta t}$, where C_{avg} is the average heat capacity.

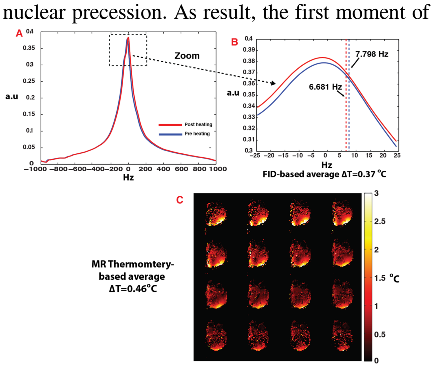

Figure 3. *In vivo* experiment. A. FIDs of the pre- and post-heating. B. Zoom onto the center frequency showing the shift in first moment. Average ΔT was 0.37 deg C. C. MR thermometry results. Average ΔT was 0.46 deg C.

METHODS: Phantom validation: A gelatin phantom was created to emulate the electrical properties of human tissue by combining 500ml of water 115.4g of Gelatin, 1g NaCl, and 0.5 g of benzoic acid. The phantom's electrical conductivity and relative permittivity were 1 S/m and 71, respectively, measured using a dielectric probe kit (Agilent 85070E, Agilent Technologies). The gel was placed inside a bottle measuring 7cm in diameter and 16.5cm in height and its thermal properties were measured using a thermal property probe (KD2 Pro, Pullman). The phantom's thermal diffusivity, thermal conductivity, heat capacity and density were 0.146 m^2/s, 0.572 W/m/K, 3660 J/kg/k and 1064 kg/m^3, respectively. A simple loop coil for heating was placed on top of the phantom (Fig. 1A) and inside a 28-element knee coil array (QED). The loop coil was tuned to 275 MHz and placed inside the coil in a 7T MRI system (Siemens Medical Solutions, Erlangen, Germany). A series of ten FIDs were acquired thirty seconds apart, after which the loop coil was connected to an RF amplifier (Kalmus, LA200UELP, Bothell, WA) delivering 74.7W of continuous power for 1 minute. After one minute of heating the sample, nine more FIDS were acquired, requiring 2 seconds each (flip angle=90 deg, matrix size= 4096, bandwidth = 2000Hz). Before and after heating a 2D interleaved spoiled gradient echo (GRE) image (TE=15 ms, TR=208 ms, 2.5x2.5x5 mm^3, flip angle=25 deg, matrix size=64x64x12 and acquisition time=13.3s) was acquired in order to validate the frequency shifts quantified using the FIDs. The first moment of the spectra of the FIDs was then calculated and a ΔT map was also reconstructed from the GRE images. In vivo: a loop coil was placed on the forearm of a subject (Fig. 1B) inside a single channel birdcage coil in the 7T scanner. A single FID was acquired with the same parameters as above followed by a GRE with the following parameters: TE=10 ms, TR=290 ms, 2.5x2.5x5 mm^3, FA=25 deg, matrix size=64x64x16 and acquisition time=18.6 s. The loop coil was then driven with 36.3W of power for 1 minute, after which second FID and GRE were acquired with the same parameters. The FIDs' first moment difference was then calculated and the ΔT map was reconstructed using the PRF method.

RESULTS: The results of the phantom experiments are shown in Fig 2, showing the average ΔT reconstructed by subtracting the first moment of the FIDs spectrum before and after heating. The difference between the FID and volume-averaged MR thermometry based measurement was 5.9%, while the standard deviation of the difference in first moment when no RF heating was applied was 0.17Hz, substantially smaller than the difference before and after heating (2.41Hz). Similarly the change in the FIDs first moment as a result of the RF power deposition is shown in Fig 2B. Fig 3 shows a comparison between the *in vivo* MR thermometry and FID results, where the difference ΔT was 19.5%.

CONCLUSION: A new method for measuring average power deposition is presented. Results are validated in a phantom and preliminary results are shown in vivo. The use of FIDs to quantify thermal dose facilitates measurement of small ΔTs, insomuch as the frequency shift caused by the thermal dose is higher than the innate B_0 changes that occur during scanning. It is important that the thermal dose is applied over a short duration of time such that heat diffusion is small and eq. (2) remains valid. Other restrictions at this time are that the signal arise mainly from water and that the receive coil have a uniform distribution over the heated region. Given these constraints, the ability to measure global RF energy coupling into the patient with this independent method should be advantageous.

REFERENCES: [1] Zhu, Y., et al. (2012), System and SAR characterization in parallel RF transmission. Magn Reson Med, 67: 1367–1378. [2] C. M. Collins et al., JMRI, vol. 19, pp. 650-6, May 2004. [3] V. Rieke et al., JMRI, vol. 27, pp. 376-90, Feb 2008.